City College of San Francisco **ASTR 20:** Introduction to
Spring 2010, Assignment # 2 Astrophysics

Due Date: February 18, 2010

Reading Assignment:

Jones & Lambourne: Chapter 2: Normal Galaxies (2.1, 2.2,& 2.3)

Supplement Reading:

Van Der Wel, et al. 2004 "The Fundamental Plane of Filed Early Type Galaxies at z = 1", **Ap.J. 601**, L5-L8

Anderssen & Bershady. 2003. " A Face-On Tully-Fisher Relation", **Ap.J. 599**, L79-L82

Problems:

1. The following are expressions for calculating the Jean's mass and Jean's radius:

$$M_J = 100T\sqrt{\frac{T}{n_H}}\ \mathfrak{M}_\odot ,$$

and

$$R_J = 10\sqrt{\frac{T}{n_H}}\ \text{pc} ,$$

where T is the temperature of the gas in kelvin, and n_H is the number of atoms per cubic centimeters. Calculate the Jean's mass and Jean's radius and identify the astronomical environments for the following conditions.

a). $n_H = 1000$ cm^{-3}, $T = 10$ K
b). $n_H = 1$ cm^{-3}, $T = 10{,}000$ K
c). $n_H = 0.1$ cm^{-3}, $T = 6{,}000$ K

2. Summarize and make comments on one of the **Ap.J. Letters.**

1. A nova binary system consists of a low mass ($0.5\mathfrak{M}_\odot$) main sequence star and a white dwarf ($1\ \mathfrak{M}_\odot$) in orbit about their common center of mass. The orbital period of such a system is typical $P \sim 4$ hours.

a). Estimate the mean orbital separation for this system. Compare the result with the radius of the Sun and with that of a $0.5\ \mathfrak{M}_\odot$ main sequence star.
b).When the nova explosion occurs, the hydrogen burning shell on the white dwarf provides a luminosity of $3 \times 10^4\ \mathfrak{L}_\odot$. Observationally, the nova at the peak of its outburst appears as a giant star of surface temperature of 10,000 K and luminosity of $3 \times 10^4\ \mathfrak{L}_\odot$. Using Stefan-Boltzmann Law, determine the radius of

the "giant" and compare it to the original dimensions of the system. Where is the main sequence companion star now?

THE ASTROPHYSICAL JOURNAL, 599:L79–L82, 2003 December 20
© 2003. The American Astronomical Society. All rights reserved. Printed in U.S.A.

A FACE-ON TULLY-FISHER RELATION

DAVID R. ANDERSEN[1]
Max Planck Institute for Astronomy, Königstuhl 17, D-69117 Heidelberg, Germany; andersen@mpia-hd.mpg.de
AND
MATTHEW A. BERSHADY
Department of Astronomy, University of Wisconsin, 475 North Charter Street, Madison, WI 53706; mab@astro.wisc.edu
Received 2003 August 4; accepted 2003 November 11; published 2003 December 12

ABSTRACT

We construct the first "face-on" Tully-Fisher (TF) relation for 24 galaxies with inclinations between 16° and 41°. The enabling measurements are integral-field echelle spectroscopy from the WIYN 3.5 m telescope, which yield accurate kinematic estimates of disk inclination to ~15°. Kinematic inclinations are of sufficient accuracy that our measured TF scatter of 0.42 mag is comparable to other surveys even without internal absorption corrections. Three of four galaxies with significant kinematic and photometric asymmetries also have the largest deviations from our TF relation, suggesting that asymmetries make an important contribution to TF scatter. By measuring inclinations below 40°, we establish a direct path to linking this scatter to the unprojected structure of disks and making nondegenerate dynamical mass decompositions of spiral galaxies.

Subject headings: galaxies: fundamental parameters — galaxies: kinematics and dynamics — galaxies: spiral — galaxies: structure

1. INTRODUCTION

One common characteristic of Tully-Fisher (TF; Tully & Fisher 1977) studies of the relation between luminosity and rotation speed is the selection of spiral galaxies with inclinations (i) above 45° and typically with $i \sim 60°$. The inability to determine accurate and precise inclinations for galaxies with $i < 40°$ has limited studies attempting to link structural parameters, such as lopsidedness and ellipticity, to TF scatter (Franx & de Zeeuw 1992; Zaritsky & Rix 1997). Likewise, combining vertical stellar velocity dispersions and disk rotation speeds has been thwarted for lack of precise inclinations for nearly face-on galaxies (e.g., Bottema 1997). Hence, nondegenerate dynamical mass decompositions of galaxies have not yet been made.

One solution to the above problems is to use nearly face-on galaxies to study the TF relation. Here the detailed planar structure of the disk can be studied unprojected, while the vertical component of the disk stellar velocity dispersion is favorably projected. The problem is now observational: how can accurate and precise inclinations be measured for small inclination angles?

For most TF studies, inclinations are calculated from photometric axis ratios, assuming circular disks, and correcting for a constant intrinsic flattening (e.g., Tully & Fouqué 1985; Courteau 1996). Bars, spiral structure, and intrinsic ellipticity cause systematic errors in photometric inclination and position angles (P.A.'s), dominate the apparent ellipticity at low inclination and skew apparent inclinations to larger values (Andersen et al. 2001; Courteau et al. 2003). Hence there is a triple penalty at low inclinations for TF studies: (1) erroneously large inclinations lead to undercorrecting the velocity projection, (2) random errors diverge since photometric disk axis ratio measurements have constant errors as a function of axis ratio, and (3) for long-slit studies, P.A. mismatch will always yield systematic underestimates of the projected rotation speed.

These pitfalls can be mitigated if kinematic inclinations are derived from two-dimensional velocity fields (e.g., Schommer et al. 1993; Verheijen 2001) because disk scale heights are irrelevant, and velocity fields between 1 and 3 scale lengths are typically less aberrated than the light distribution by spiral structure, bars, or warps (Courteau et al. 2003; Briggs 1990). A limit of ~40° had been set on the minimum derived kinematic inclinations for nearby galaxies from H I maps (Begeman 1989), but this minimum value is not fundamental; it is notionally adopted as such.

We have discovered that kinematic inclinations, derived from high-quality optical kinematic data collected with integral field units, are sufficiently accurate and precise to construct a TF relation at inclinations as low as 15°. In this Letter we present an analysis of the first TF relation for a sample of nearly face-on galaxies.

2. THE PHOTOMETRIC AND KINEMATIC DATA SET

We obtained R- and I-band images and Hα velocity fields of 39 spiral galaxies meeting the criteria of Andersen et al. (2001): galaxies appear nearly face-on ($i < 30°$), are of intermediate type (Sab–Sd), with no clear signs of interactions, bars, or rings, and are in regions of low Galactic extinction. Our sample and observations are described in Andersen (2001).

CCD images were acquired over 17 nights between 1998 May and 2001 January at the WIYN 3.5 m,[2] the KPNO 2.1 m, and the McDonald Observatory 2.7 m telescopes. Total magnitudes are defined as asymptotic fluxes, as measured from growth curves, calibrated on the Kron-Cousins system using Landolt (1983) standards observed on four photometric nights. Zero points for other nights are internally boot-strapped, where possible, from repeat observations. We use $H_0 = 70$ km s^{-1} Mpc^{-1} and correct magnitudes for Galactic absorption (Schlegel, Finkbeiner, & Davis 1998). (Virgo in-fall affects recession velocities by <1%; Paturel et al. 1997.) We use the mean $R-I$ color of 0.52 ± 0.08 mag for our calibrated sample to estimate the R magnitude for several galaxies with only accurate I-band

[1] Visiting Astronomer, Kitt Peak National Observatory, National Optical Astronomy Observatory, which is operated by the Association of Universities for Research in Astronomy (AURA), Inc., under cooperative agreement with the National Science Foundation.

[2] The WIYN Observatory is a joint facility of the University of Wisconsin at Madison, Indiana University, Yale University, and NOAO.

photometry and add the 0.08 mag range in $R-I$ in quadrature as an additional uncertainty for these sources.

Hα velocity fields were obtained at an instrumental resolution of $\lambda/\Delta\lambda \approx 13{,}000$ using the DensePak integral field unit (Barden, Sawyer, & Honeycutt 1998) on the WIYN 3.5 m telescope over 11 nights between 1998 May and 2000 January. (PGC 56010, a low surface brightness galaxy, was reobserved using SparsePak [Bershady et al. 2003] in 2001 May.) The Hα emission lines were resolved, with typical signal-to-noise ratio levels of ~35 and centroid precision of ~1.5 km s^{-1}. DensePak observations yield velocity centroids for ~140 independent positions within each galaxy out to 2.2–5.8 disk scale lengths (typically 3.3).

3. MEASURING INCLINATIONS BELOW 40°

The most critical measurement required to construct a "face-on" TF (FOTF) relation is the derivation of accurate and precise disk inclinations. As we have argued, there are fundamental reasons that two-dimensional kinematic maps provide the only viable data for measuring these inclinations. Using a method similar to that described in Andersen et al. (2001), we fit the DensePak data with a single hyperbolic tangent velocity-field model. From these fits, we derive measurements of kinematic inclinations, rotation speeds ($V_{\rm rot}$), and recession velocities for our sample.

Of the 39 galaxies in our sample, we measure reliable deprojected rotation velocities, $V_{\rm circ} \equiv V_{\rm rot}/\sin i$, for 26 (see Table 1; two galaxies lacking calibrated R- and I-band magnitudes are excluded). This subsample has $V_{\rm rot} < 120$ km s^{-1} with inclinations and errors from 16^{+5}_{-10} to 41^{+5}_{-6} degrees. Ten additional galaxies have measured, deprojected rotation velocities but kinematic inclinations consistent with zero within 68% confidence intervals. Their mean inclination is 8°. Three remaining galaxies have no projected circular velocity field; they appear truly face-on. Our results paint a consistent picture of being able to measure inclinations reliably down to $i \sim 15°$.

Why can we measure accurate inclinations for nearly face-on galaxies? For disks with inclinations between 20° and 30°, the peak difference in projected velocity is only 2–3 km s^{-1} between disks with inclinations differing by 5°. To measure this difference requires less than 2 km s^{-1} centroiding precision per fiber, or many samples of the velocity field at a precision at least comparable to this difference. The latter, which we achieve, is preferable because of random motions. We find typically 3 km s^{-1} rms variations between our model and the data (Andersen 2001).

Historically, H I data have been claimed to be of insufficient quality for deriving galaxy inclinations below 40° (Begeman 1989). One aspect of the problem has been that tilted ring models include a weighting scheme that, when typically implemented, minimizes the importance of velocity measurements at azimuthal angles that are most influenced by changes in inclination. For example, Begeman's simulations use a $\cos\theta$ weighting scheme, where θ is the angle from the major axis in the galaxy plane. This weighting is done to minimize the effects of warps, but in so doing over half of the signal is thrown out. For the same reason, data are often not considered beyond θ of 30° or 45°, throwing out yet more of the signal.

Our DensePak observations sample the inner disks of galaxies, where warps tend to be negligible. Hence we can use the entire velocity field to maximize the influence of inclination in the model velocity fields. Figure 1 shows deprojected position-velocity diagrams for two representative galaxies in different bins of θ. Excellent agreement between azimuthal bins indicates a good model fit and lack of systematics. We find bidimensional echelle spectroscopy to be of sufficient quality to yield deprojected rotation velocities, $V_{\rm rot}/\sin i$ at precisions better than 10% at inclinations above 28°; a 20% precision on $V_{\rm rot}/\sin i$ is reached for inclinations of ~20°.

TABLE 1

TULLY-FISHER PARAMETERS

PGC	i (deg)	$V_{\rm circ}$ (km s^{-1})	M_R (mag)
2162	$25.8^{+5.2}_{-6.6}$	$81.2^{+38.5}_{-30.4}$	-20.42 ± 0.03
3512	$30.1^{+2.3}_{-2.7}$	$164.3^{+26.7}_{-22.8}$	-21.17 ± 0.03
5673	$21.0^{+3.2}_{-5.0}$	$160.6^{+72.6}_{-46.5}$	-20.89 ± 0.05
6855[a]	$38.8^{+3.2}_{-3.8}$	$84.3^{+14.0}_{-11.8}$	-20.64 ± 0.05
7826[b]	$40.7^{+3.2}_{-3.8}$	$49.0^{+11.2}_{-8.3}$	-19.30 ± 0.06
14564[a]	$30.5^{+2.9}_{-3.1}$	$181.8^{+33.4}_{-31.2}$	-21.48 ± 0.05
16274	$30.6^{+2.3}_{-2.7}$	$222.4^{+35.4}_{-30.2}$	-22.03 ± 0.05
23333	$26.9^{+3.8}_{-4.5}$	$133.0^{+40.9}_{-34.6}$	-20.67 ± 0.06
23598	$16.2^{+5.2}_{-9.8}$	$162.3^{+189.8}_{-100.7}$	-21.69 ± 0.05
24788[a]	$41.5^{+4.9}_{-6.2}$	$112.8^{+27.4}_{-21.7}$	-21.70 ± 0.05
26140	$28.2^{+3.0}_{-4.3}$	$317.3^{+88.1}_{-61.6}$	-22.86 ± 0.05
28310	$35.3^{+2.8}_{-3.2}$	$110.9^{+17.5}_{-15.3}$	-20.38 ± 0.07
31159[a]	$22.6^{+3.0}_{-4.0}$	$220.1^{+73.4}_{-55.0}$	-21.19 ± 0.07
32638	$22.0^{+3.7}_{-4.9}$	$234.25^{+98.4}_{-74.4}$	-21.80 ± 0.05
33465	$18.6^{+4.1}_{-5.6}$	$309.8^{+178.6}_{-130.8}$	-22.41 ± 0.05
36925	$22.6^{+3.5}_{-4.5}$	$195.2^{+73.2}_{-57.0}$	-22.06 ± 0.07
38908	$26.0^{+3.6}_{-4.0}$	$211.0^{+60.3}_{-54.3}$	-21.96 ± 0.06
39728[b]	$31.8^{+3.3}_{-3.6}$	$144.2^{+29.2}_{-26.8}$	-20.32 ± 0.06
46767	$22.7^{+2.6}_{-3.0}$	$288.2^{+43.4}_{-50.6}$	-22.79 ± 0.07
56010	$26.7^{+8.3}_{-13.6}$	$75.3^{+70.7}_{-43.2}$	-19.97 ± 0.07
57931	$21.5^{+4.0}_{-5.3}$	$192.4^{+90.0}_{-68.0}$	-21.83 ± 0.05
58410	$29.0^{+2.0}_{-2.5}$	$231.4^{+36.3}_{-29.1}$	-22.11 ± 0.10
72144	$27.9^{+4.2}_{-5.9}$	$110.6^{+42.8}_{-30.6}$	-21.27 ± 0.03
72453	$21.2^{+4.0}_{-6.6}$	$212.4^{+125.6}_{-76.3}$	-22.23 ± 0.03

[a] Significant photometric and kinematic asymmetry.

[b] $V_{\rm heliocentric} < 3000$ km s^{-1}.

4. FOTF VERSUS CONVENTIONAL TF RELATIONS

To evaluate our FOTF data set, we compare it to the TF samples of Courteau (1997) and Verheijen (2001). The salient difference between our sample versus Courteau's and Verheijen's is that their galaxies have $i > 40°$ and $\bar{i} \sim 65°$. Courteau's sample shares comparable scale lengths, colors, surface brightnesses, and distances and uses spatially resolved Hα long-slit emission as the kinematic tracer. We use the cleaner "quiet Hubble flow" subset of Courteau's sample and convert Courteau's Lick r-band photometry to Cousins R band using $R - r = -0.36$ (Fukugita, Shimasaku, & Ichikawa 1995). Verheijen collected multiband (including Cousins R band) photometry and H I synthesis maps for a volume-limited sample from the nearby Ursa Major Cluster. We select the Ursa Major subsample with $M_R < -19$, corresponding to the faint end of the FOTF and Courteau samples, and adopt the *Hubble Space Telescope* Key Project distance (Sakai et al. 2000). Both Courteau and Verheijen use an internal-absorption correction of the form $A_i = \gamma \log a/b$ that minimizes the apparent TF scatter. (We have subtracted from Courteau's data his zero-point correction of 0.40 mag, which corresponds to his absorption correction at $i = 70°$.) Since our sample is nearly face-on, we apply no internal-absorption corrections to our photometry.

An inspection of the three samples in M_R versus $\log(2V_{\rm rot}/\sin i)$ of Figure 2 highlights the differences and similarities in their TF relations. There is excellent agreement between the Courteau and Verheijen TF slopes and zero points. There is also an excellent agreement in the zero point of the FOTF with Verheijen and Courteau TF relations near L^* at

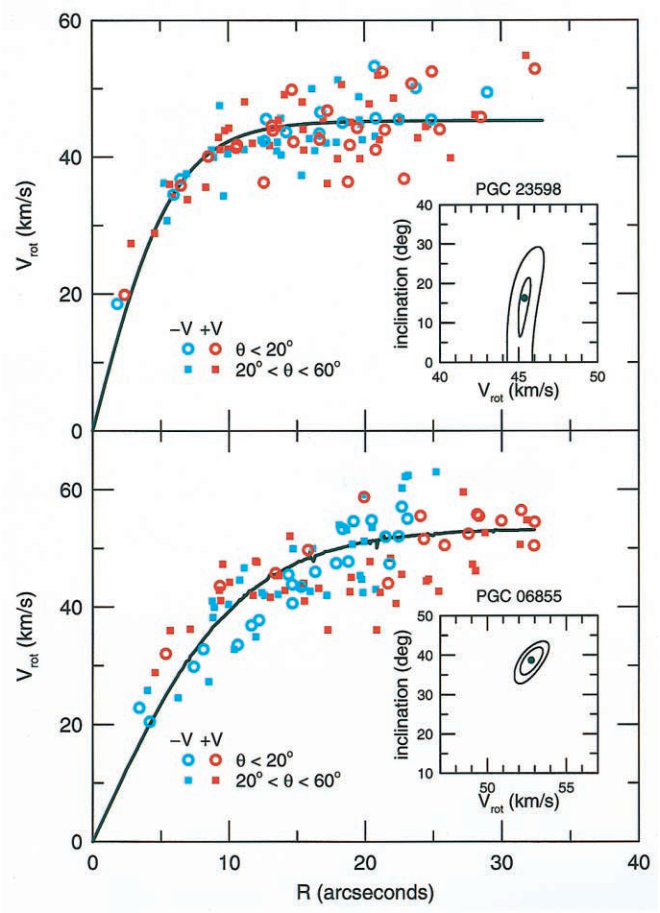

FIG. 1.—Azimuthally deprojected position-velocity diagram for PGC 23598 (*top*) and PGC 6855 (*bottom*). Each datum is a separate fiber measurement. Velocities, color coded as receding (*red*) or approaching (*blue*), are marked as open circles for $\theta < 20°$ and filled squares for $20° < \theta < 60°$. Solid curves trace the projected *model* rotation curve along the major axis; χ^2 maps of the 68% and 90% confidence limits on model inclination and rotation velocity are inset. PGC 6855 is photometrically lopsided and kinematically disturbed; it falls well off the TF relation (Fig. 2). PGC 23598 has the lowest sample inclination but falls directly on the TF relation.

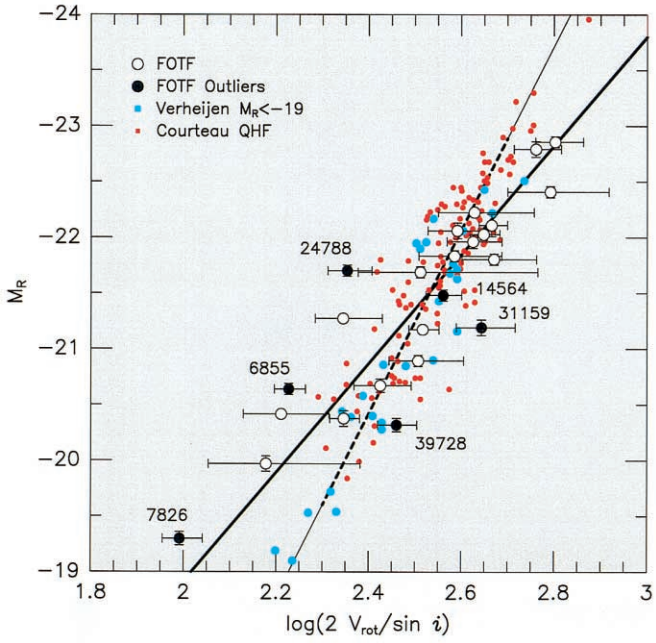

FIG. 2.—TF relations for our sample of galaxies with $\bar{i} = 26°$ (FOTF, *white and black*) and more-inclined samples of Courteau (1997; *red*) and Verheijen (2001; *blue*). FOTF "outliers" (*filled circles*) are defined in text and Table 1. The heavy solid line with slope −4.90 is the best fit to the FOTF data (with or without outliers) using a backward regression that allows for intrinsic scatter and heteroscedastic errors (bivariate correlated errors and intrinsic scatter [BCES] [X|Y]; Akritas & Bershady 1996). The heavy dashed line is the best fit to the FOTF sample between $2.3 < \log V_{\rm rot} < 2.7$; it is indistinguishable from the best fits to Courteau and Verheijen (*light solid line with slope* −8.2).

$M_R \sim -22$, but the shallower slope of the FOTF appears striking. However, slopes vary between −7 and −9 for both the Courteau and the Verheijen samples depending on the method of velocity measurement, the extinction correction prescription, and the sample selection. Verheijen (2001) notes that the above absorption corrections steepen TF slopes. However, these corrections do not alter the slope of the FOTF relation. While empirical corrections (e.g., Giovanelli et al. 1994; Tully et al. 1998) work well for galaxies with $40° < i < 80°$, the corrections for galaxies with $i < 30°$ are small ($A_R \sim 0.1$ mag). Since in practice one can systematize velocity measurements, a larger FOTF spanning a broader range in luminosity may provide a new test of the veracity of TF-based internal extinction corrections.

When we restrict our sample by luminosity or $V_{\rm rot}$, we find slopes between −5 and −8; a FOTF subsample with $2.3 < \log (2V_{\rm circ}) < 2.7$ shares the same slopes and zero points as the Courteau and Verheijen culled samples (Fig. 1). This implies that only the extreme rotators, fast and slow, differ. This may be due to luminosity-dependent extinction corrections discussed above. It is more difficult to present a plausible systematic error whereby the high luminosity objects rotate faster and the low luminosity objects rotate slower and the intermediate objects are unaffected. However, with only six galaxies in these regimes, the discrepancy between slopes may be influenced by our small-number statistics coupled with relatively large errors on $\log V/\sin i$.

If the FOTF is to be a useful tool for studying internal extinction or, e.g., correlations of galaxy properties to TF scatter, the impact of inclination measurements on TF residuals needs to be examined. Figure 3 shows the relation between TF residuals and inclination along with the predicted envelope of TF residuals introduced by inclination error. We find that the scatter for our sample is comparable to the scatter in the culled Courteau and Verheijen samples: 0.42 mag for ours versus 0.38 mag for the Verheijen and Courteau samples used here, each about their respective regressions (Fig. 2). Six galaxies labeled in Figures 2 and 3 are noted in Table 1 as either being photometrically or kinematically asymmetric or having small recession velocities (hence uncertain distances). Inclination errors alone are not the cause of their large TF residuals. Removing these six galaxies, the scatter for our face-on sample about its shallow regression drops significantly to 0.3 mag and is consistent with our measurement errors.

5. SUMMARY AND DISCUSSION

We have presented a TF relationship for 24 galaxies with a mean inclination of 26°—the first time the TF relation has been measured for a sample of galaxies with inclinations less than 40°. Accurate and precise kinematic inclinations are the key to studying TF relation at low inclination, and velocity fields are the essential ingredient for their measurement. We are able to construct this FOTF relation from integral-field Hα velocity fields for four primary reasons: (1) DensePak and SparsePak are efficient for gathering Hα velocity fields with moderately

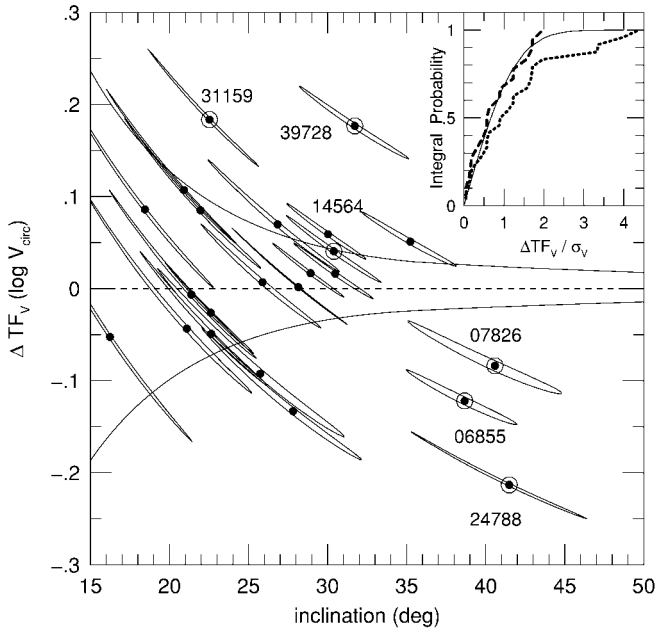

FIG. 3.—TF residuals vs. inclination for sample galaxies. 68% confidence limits on each galaxy reflect uncertainty in kinematic inclination and rotation velocity propagated through the best-fit TF relation. The envelope defined by the two solid curves encloses the area in which 68% of points are expected to fall if *all* TF scatter were due solely to uncertainties in kinematic inclinations. "Outlier" galaxies (see text and Table 1) are labeled. That five of the six labeled galaxies fall outside the envelope suggests that factors besides inclination errors make these galaxies TF outliers.

high spatial resolution and medium spectral resolution at high signal-to-noise ratio, (2) Hα velocity fields generally extend out to ~3 disk scale lengths so that warping, which dominates the outer radii of some galaxy disks, is unimportant, (3) instead of using multiple tilted rings, we successfully fit galaxy disks with a single velocity-field model, simultaneously using data at all radii and phase angles, and (4) we equally weight all data, making our fits sensitive to the signal constraining inclination, which peaks in the velocity field at ~45° from the major axis.

The FOTF relation measured from our data has a zero point and scatter comparable to conventional TF relations but possibly a shallower slope. The bulk of the FOTF scatter is consistent with measurement errors, as found by Verheijen (2001). Of the four galaxies that show large kinematic and photometric asymmetries, three fall well off the TF relation. While our statistics are small, this is consistent with the claim by Barton et al. (2000) that kinematic asymmetries are an important source of TF scatter.

The FOTF can play an important role in understanding the nature and interpretation of the TF slope, zero point, and scatter in three ways. First, internal extinction is less important for face-on galaxies minimizing inclination-dependent effects. For inclined TF samples, if correlated errors exist between dereddened luminosities and deprojected rotation speeds, TF scatter will be increased. If extinction depends on luminosity or velocity (mass), the corrected TF slopes may differ from their true values.

Second, measurements of asymmetry, ellipticity, and lopsidedness ideally are made at low inclinations. Several studies have suggested that nonaxisymmetric dark halo mass distributions such as lopsidedness (Zaritsky & Rix 1997; Swaters et al. 1999) or ellipticity (Franx & de Zeeuw 1992; Andersen et al. 2001) could be sources of TF scatter. However, without access to inclination measurements for face-on systems, these claims could not be directly evaluated. Our small FOTF sample suggests that such links are possible and show that such studies can now be pursued wholesale.

Finally, the mass-to-light ratio of spiral disks is an essential ingredient for interpreting the TF zero point, slope, and scatter. Only limits can be placed on mass decompositions (Bell & de Jong 2001) without direct dynamical estimates of total *and* disk mass. This can be accomplished via rotation curves *and* vertical stellar velocity dispersions of disks. The latter are best measured in face-on systems, and hence the FOTF unlocks the door for determining the fundamental mass budget of spiral galaxies.

We thank E. Bell, S. Courteau, and B. Tully for helpful comments. We acknowledge NSF AST 99-70780 and AST 03-07417.

REFERENCES

Akritas, M. G., & Bershady, M. A. 1996, ApJ, 470, 706
Andersen, D. R. 2001, Ph.D. thesis, Pennsylvania State Univ.
Andersen, D. R., Bershady, M. A., Sparke, L. S., Gallagher, J. S., & Wilcots, E. M. 2001, ApJ, 551, L131
Barden, S. C., Sawyer, D. G., & Honeycutt, R. K. 1998, Proc. SPIE, 3355, 892
Barton, E. J., Geller, M. J., Bromley, B. C., van Zee, L., & Kenyon, S. J. 2001, AJ, 121, 625
Begeman, K. 1989, A&A, 223, 47
Bell, E. F., & de Jong, R. S. 2001, ApJ, 550, 212
Bershady, M. A., Andersen, D. R., Verheijen, M. A. W., Westfall, K. B., Crawford, S. M., & Swaters, R. A. 2003, ApJS, submitted
Bottema, R. 1997, A&A, 328, 517
Briggs, F. H. 1990, ApJ, 352, 15
Courteau, S. 1996, ApJS, 103, 363
———. 1997, AJ, 114, 2402
Courteau, S., Andersen, D. R., Bershady, M. A., MacArthur, L. A., & Rix, H.-W. 2003, ApJ, 594, 208
Franx, M., & De Zeeuw, T. 1992, ApJ, 392, L47
Fukugita, M., Shimasaku, K., & Ichikawa, T. 1995, PASP, 107, 945
Giovanelli, R., Haynes, M. P., Salzer, J. J., Wegner, G., da Costa, L. N., & Freudling, W. 1994, AJ, 107, 2036
Landolt, A. U. 1983, AJ, 88, 853
Paturel, G., et al. 1997, A&AS, 124, 109
Sakai, S., et al. 2000, ApJ, 529, 698
Schlegel, D. J., Finkbeiner, D. P., & Davis, M. 1998, ApJ, 500, 525
Schommer, R. A., Bothun, G. D., Williams, T. B., & Mould, J. R. 1993, AJ, 105, 97
Swaters, R. A., Schoenmakers, R. H. M., Sancisi, R., & van Albada, T. S. 1999, MNRAS, 304, 330
Tully, R. B., & Fisher, J. R. 1977, A&A, 54, 661
Tully, R. B., & Fouqué, P. 1985, ApJS, 58, 67
Tully, R. B., Pierce, M. J., Huang, J.-S., Saunders, W., Verheijen, M. A. W., & Witchalls, P. L. 1998, AJ, 115, 2264
Verheijen, M. A. W. 2001, ApJ, 563, 694
Zaritsky, D., & Rix, H.-W. 1997, ApJ, 477, 118

THE ASTROPHYSICAL JOURNAL, 601:L5–L8, 2004 January 20
© 2004. The American Astronomical Society. All rights reserved. Printed in U.S.A.

THE FUNDAMENTAL PLANE OF FIELD EARLY-TYPE GALAXIES AT $z = 1$[1]

A. VAN DER WEL,[2] M. FRANX,[2] P. G. VAN DOKKUM,[3] AND H.-W. RIX[4]

Received 2003 October 3; accepted 2003 December 8; published 2004 January 19

ABSTRACT

We present deep VLT spectra of early-type galaxies at $z \approx 1$ in the Chandra Deep Field–South, from which we derive velocity dispersions. Together with structural parameters from *Hubble Space Telescope* imaging, we can study the fundamental plane for field early-type galaxies at that epoch. We determine accurate mass-to-light ratios (*M/L*) and colors for four field early-type galaxies in the redshift range $0.96 < z < 1.14$, and two with $0.65 < z < 0.70$. The galaxies were selected by color and morphology, and have generally red colors. Their velocity dispersions show, however, that they have a considerable spread in *M/L* (by a factor of 3). We find that the colors and directly measured *M/L* correlate well, demonstrating that the spread in *M/L* is real and reflects variations in stellar populations. The most massive galaxies have *M/L* comparable to massive cluster galaxies at similar redshift and therefore have stellar populations that formed at high redshift ($z > 2$). The lower mass galaxies at $z \approx 1$ have a lower average *M/L*, and one is a genuine "E+A" galaxy. The *M/L* indicate that their luminosity-weighted ages are a factor of 3 younger at the epoch of observation, because of either a low formation redshift or late bursts of star formation contributing 20%–30% of the mass.

Subject headings: cosmology: observations — galaxies: evolution — galaxies: formation

1. INTRODUCTION

Good understanding of the formation and evolution of early-type galaxies is one of the major challenges for current structure-formation models. Models of hierarchical structure generally predict that field early-type galaxies form relatively late (e.g., Diaferio et al. 2001). One of the prime diagnostics of the formation history of early-type galaxies is the evolution of the *M/L* as measured from the fundamental plane (FP; Franx 1993). Studies of the evolution of the luminosity function, together with the evolution of *M/L*, quantify the evolution of the mass function. Previous studies of the evolution of the *M/L* have produced consistent results for the evolution of massive cluster early-type galaxies: the evolution is slow, consistent with star formation redshifts $z \approx 2$ (e.g., van Dokkum & Stanford 2003).

On the other hand, studies of the evolution of field galaxies have yielded more contradictory results: whereas early studies found slow evolution (e.g., van Dokkum et al. 2001; Treu et al. 2001; Kochanek et al. 2000), more recently, evidence for much faster evolution was found by Treu et al. (2002) and Gebhardt et al. (2003); and yet other authors found that the majority of field early-types evolve slowly, with a relatively small fraction of fast-evolving galaxies (e.g., Rusin et al. 2003; van Dokkum & Ellis 2003; van de Ven, van Dokkum, & Franx 2003; Bell et al. 2003).

These previous measurements suffered from several uncertainties: the signal-to-noise ratios (S/Ns) of the spectra were generally quite low, much lower than usual for nearby studies of the FP (e.g., Faber et al. 1989; Jørgensen et al. 1996). Those studies, based on lensing galaxies, used stellar-velocity dispersions derived from image separations.

In this Letter, we present high-S/N spectra and accurate measurements of the *M/L* of four field elliptical galaxies with $z = \sim 1$–1.14 and two at $z \sim 0.7$ in the Chandra Deep Field–South (CDF-S). The S/Ns are comparable to those obtained for nearby galaxies. Together with accurate multiband photometry available for the CDF-S, we have measured the accurate *M/L* and rest-frame optical colors at $z \sim 1$.

Throughout this Letter we use Vega magnitudes and assume a Λ-dominated cosmology ($[\Omega_M, \Omega_\Lambda] = [0.3, 0.7]$), with a Hubble constant of $H_0 = 70$ km s^{-1} Mpc^{-1}.

2. SPECTROSCOPY

2.1. *Sample Selection and Observations*

The galaxies were selected from the COMBO-17 catalog (see Wolf et al. 2003), and imaging was obtained by the Great Observatories Origin Deep Survey[5] (GOODS; data release ver. 0.5) from the Advanced Camera for Surveys (ACS) on the *Hubble Space Telescope*. We selected compact, regularly shaped galaxies with photometric redshifts higher than 0.8 and $I-z \geq (I-z)_{\rm Sbc}$, $z < 22$. $(I-z)_{\rm Sbc}$ denotes the color of the Sbc template of Coleman, Wu, & Weedman (1980) at the photometric redshift. This template has $(U-V)_{z=0} = 0.95$. The typical uncertainty in the color is 0.1 mag. Lower priority galaxies were included with either lower redshifts or later types.

The CDF-S was observed in MXU mode with FORS2 on VLT-UT4 during three runs from 2002 September through 2003 February, for a total of 14 hr. The 600 *z* grism (central wavelength 9010 Å, resolution 5.1 Å or $\sigma_{\rm instr} = 72$ km s^{-1}) was used. During the observations toward the CDF-S the seeing varied between 0.″7 and 1.″5, with a median seeing of about 1″. The sky was clear all the time.

2.2. *Velocity Dispersions*

It turned out that 10 out of the 11 high-priority objects at $z_{\rm phot} \sim 1$ have the spectrum of a quiescent galaxy; the other one has a bright [O II] emission line. The brightest four ($z \lesssim 21.0$, independent of the color) had sufficient S/Ns to perform reliable dispersion measurements. The rest-frame spectra of these four galaxies are shown in Figure 1. They all show

[1] Based on observations collected at the European Southern Observatory, Chile (169.A-0458).

[2] Leiden Observatory, P.O. Box 9513, J. H. Oort Building, Niels Bohrweg 2, NL-2300 RA, Leiden, Netherlands.

[3] Department of Astronomy, Yale University, P.O. Box 208101, New Haven, CT 06520-8101.

[4] Max-Planck-Institut für Astronomie, Königstuhl 17, D-69117 Heidelberg, Germany.

[5] See http://www.stsci.edu/science/goods.

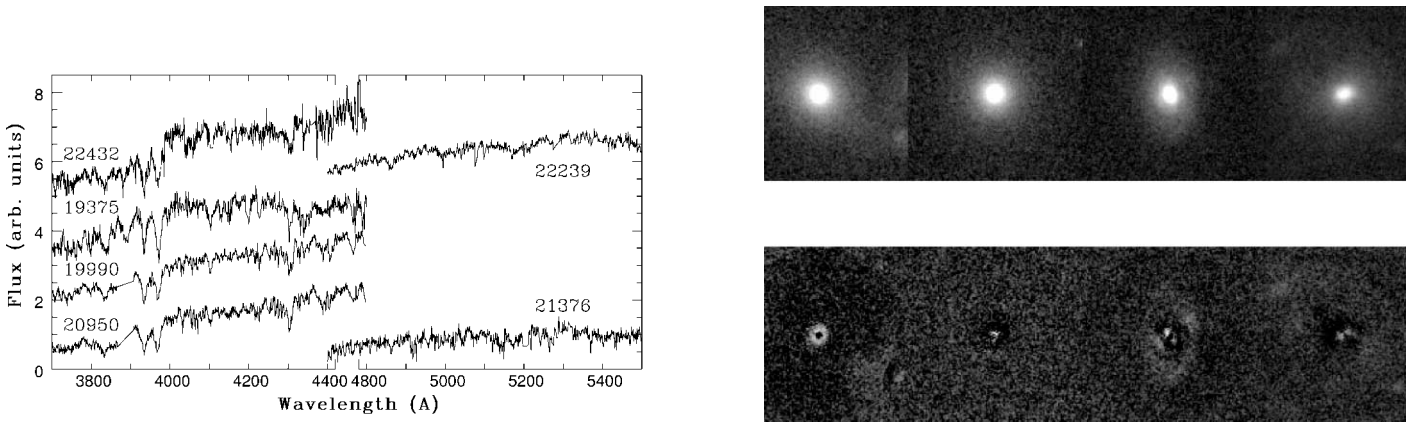

FIG. 1.—*Left*: Unsmoothed rest-frame spectra of the six objects with velocity dispersions. Regions with bright sky lines are interpolated. The wavelength scale is interrupted at $\lambda = 4500$ Å. *Right*: ACS images (F850LP) of the four galaxies at $z \sim 1$, and the residual images from the $r^{1/4}$ fit. *From left to right*: 20950, 19990, 19375, and 22432.

a strong 4000 Å break and Ca lines. Balmer lines (especially the Hδ line) are also present, although varying in strength from object to object (see Table 1). Object 19375 is an "E+A" galaxy, according to the criteria used by Fisher et al. (1998). For two ellipticals with $0.65 < z < 0.70$ we also have sufficient signal to determine a velocity dispersion.

Dispersions were measured by convolving a template star spectrum to fit the galaxy spectrum as outlined by van Dokkum & Franx (1996). We tested this procedure extensively, using different template stars and masking various spectral regions. The final values for the velocity dispersions (see Table 1) were obtained by masking the Ca H and K and Balmer lines and using the best-fitting template spectrum, which was a high-resolution solar model spectrum[6] smoothed and rebinned to match the resolution of the galaxy spectra. The Ca lines were not included in the fit because this greatly reduced the dependence of the measured velocity dispersions on template type. The tests using different templates and different masking of the Ca lines indicate that the systematic uncertainty is ~5%.

In order for the results to be comparable to previous studies, an aperture correction as described by Jørgensen, Franx, & Kjærgaard (1995b) was applied to obtain velocity dispersions within a circular aperture with a radius of 1.″7 at the distance of the Coma Cluster. This correction is ~7%.

This is the first extensive sample of such objects at $z > 0.9$ with high S/N (see van Dokkum & Ellis 2003; Treu et al. 2002; Gebhardt et al. 2003, for other spectroscopic studies).

[6] See http://bass2000.obspm.fr.

3. PHOTOMETRY

Photometry and structural parameters were determined from the GOODS ACS images (data release ver. 1.0). Images are available in four filters (F435W, F606W, F775W, and F850LP), which we refer to as *b*, *v*, *i*, and *z*, respectively.

For each object, the effective radius (r_e) and the surface brightness at the effective radius (μ_e) were obtained by fitting an $r^{1/4}$ profile, convolved by the point-spread function (PSF; van Dokkum & Franx 1996); *z*-band images were used for the $z \sim 1$ objects, and *i*-band images for the $z \sim 0.7$ objects. Stars were used as the PSF. The resulting values for r_e and μ_e vary by ≈10% when using different stars, but also correlate such that the error is almost parallel to the FP (van Dokkum & Franx 1996). Therefore, the errors in our results are dominated by the errors in the velocity dispersions. The results are listed in Table 1. The images of the $z \sim 1$ objects and the residuals of the fits are shown in Figure 1.

To determine the $i-z$ and $v-i$ colors, fluxes were calculated from the $r^{1/4}$ model within the measured effective radius. To this model flux we added the flux within the same radius in the residual images. We corrected for Galactic extinction based on the extinction maps from Schlegel, Finkbeiner, & Davis (1998). The correction is extremely small: $E(B-V) = 0.007$.

Rest-frame *B*-band surface brightnesses and rest-frame $U-V$ colors were obtained by transforming observed flux densities in two filters to a rest-frame flux density exactly as outlined by van Dokkum & Franx (1996). The spectral energy distribution used to calculate the transformations is the early-type spectrum from Coleman et al. (1980). We found the same

TABLE 1
PHOTOMETRIC AND SPECTROSCOPIC PROPERTIES

ID	α (arcsec)	δ (arcsec)	z_{spec}	i	$v-i$	$i-z$	log r_e (kpc)	μ_e	S/N (Å^{-1})	σ (km s^{-1})	(Hγ + Hδ)/2 (Å)	[O II] (Å)
19375	0	−50	1.089	21.72	1.71	1.04	−0.410 ± 0.012	21.75 ± 0.05	26	198 ± 25	4.1	−4.6
19990	−32	−35	0.964	21.32	1.89	1.00	−0.388 ± 0.007	21.45 ± 0.03	49	159 ± 14	2.5	>−1
20950	−73	−6	0.964	21.18	2.07	1.07	0.0085 ± 0.026	22.95 ± 0.08	39	261 ± 23	<1	>−1
22432	83	41	1.135	22.38	2.00	1.42	−0.109 ± 0.040	23.35 ± 0.13	21	217 ± 20	<1	−4.4
21376	129	10	0.685	21.46	1.77	0.58	−0.447 ± 0.001	22.16 ± 0.04	27	156 ± 24	…	…
22239	236	35	0.660	20.67	1.67	0.50	−0.842 ± 0.002	19.83 ± 0.03	40	177 ± 19	…	…

NOTE.—Coordinates are in arcseconds east and north of R.A. = $03^h32^m25^s$, decl. = $-27°54'00''$. Errors in the magnitudes and colors are, respectively, 0.03 and 0.05 mag. Effective radii and surface brightnesses (mag arcsec^{-2} at r_e) are measured in the *z*-band for objects 19375, 19990, 20950, and 22432, and in the *i*-band for objects 21376 and 22239. The listed errors in the velocity dispersions are fitting errors and do not include a 5% systematic error.

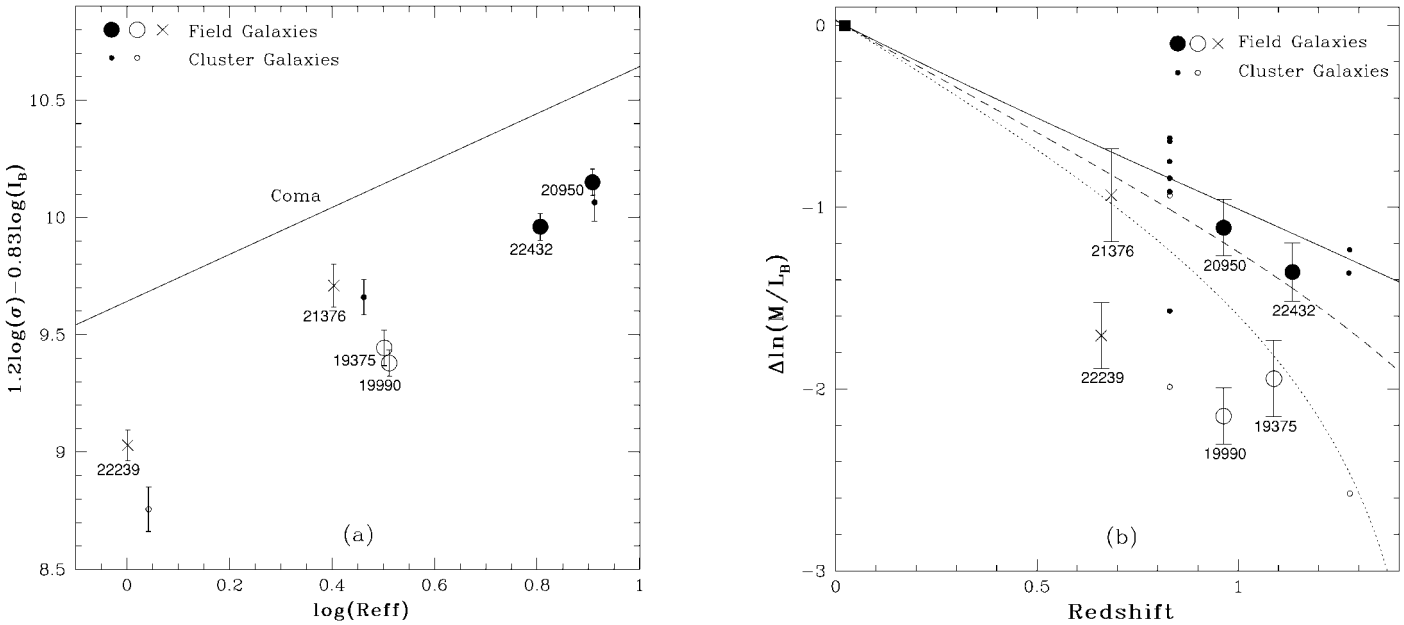

FIG. 2.—(*a*) FP points of the field galaxies presented in this paper (errors include a 5% systematic effect in the velocity dispersions), the FP points of cluster galaxies at $z = 1.27$ (van Dokkum & Stanford 2003), and the FP of the Coma Cluster (Jørgensen et al. 1996). (*b*) Offsets in M/L_B from the Coma Cluster FP (*square*; derived from Jørgensen et al. 1996). Besides the $z = 1.27$ cluster, this figure also contains the data from van Dokkum et al. (1998) on the MS 1054 cluster at $z = 0.83$. The full, dashed and dotted curves are the model predictions for a single burst of star formation with a Salpeter (1955) initial mass function for redshifts 3, 2, and 1.5, respectively. Filled symbols indicate galaxies with masses $M > 3 \times 10^{11}\ M_\odot$; other symbols indicate galaxies less massive than that. Crosses and squares distinguish between galaxies at $z < 0.8$ and $z > 0.8$, respectively. All galaxies occupying the region below the $z = 1.5$ model curve are "E+A" galaxies, except 19990, and have masses less than $3 \times 10^{11}\ M_\odot$. The more massive galaxies have significantly older stellar populations.

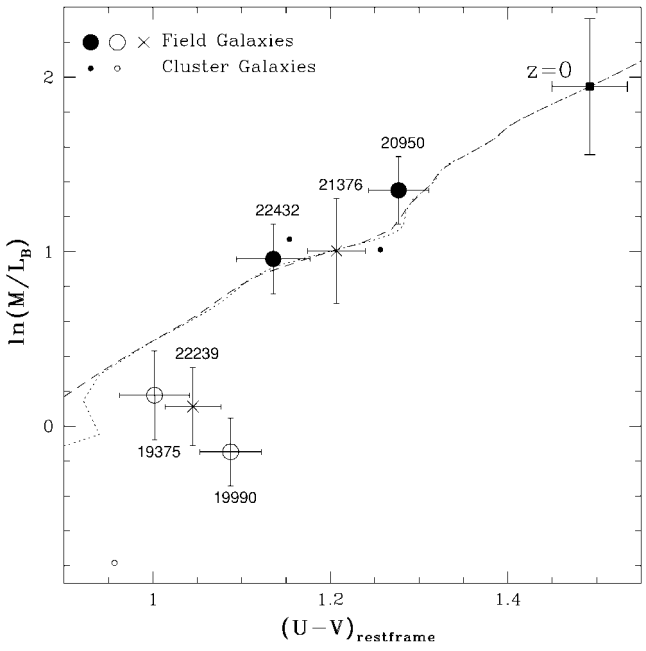

FIG. 3.—Rest-frame $U-V$ color vs. M/L_B in solar units. Filled symbols are objects more massive than $M > 3 \times 10^{11}\ M_\odot$; open symbols represent the less massive ones. The cluster galaxies are the $z = 1.27$ galaxies from Fig. 2. The redshift zero data point is the average for galaxies with $\sigma > 150$ km s^{-1} in the clusters Abell 194 and DC 2345−28 (Jørgensen, Franx, & Kjærgaard 1995a). The lines are solar-metallicity Bruzual & Charlot (2003) models with constant star formation during the first 200 Myr (*dotted line*) and exponentially decaying star formation on the same timescale (*dashed line*).

results for other template spectra. The results are listed in Table 1.

4. MASS-TO-LIGHT RATIOS FROM THE FUNDAMENTAL PLANE

Figure 2*a* shows the FP for the six field galaxies described above, and the FP for Coma derived by Jørgensen et al. (1996). Additionally, we show the results from van Dokkum & Stanford (2003) on three cluster galaxies at $z = 1.27$. The offsets of the high-redshift galaxies from the Coma FP are a measure of the evolution of *M/L*. We show the evolution of *M/L* in Figure 2*b* as a function of redshift.

Obviously, the field galaxies at $z > 0.6$ span a wide range in offsets, by a factor of approximately 3 in *M/L*. The error bars on the individual points are much smaller than the offsets. A model with a single-formation redshift can be ruled out at the 99% confidence level, as measured from the χ^2 method. The rest-frame colors of the galaxies confirm the reality of the variations in the *M/L*. As shown in Figure 3, a very strong correlation exists between the colors and the *M/L*, in the direction predicted by population synthesis models. The good correlation demonstrates that colors can be used to estimate the *M/L*, as applied, for example, by Bell et al. (2003), to a large sample of field early-type galaxies.

We note that galaxies in our study lie fairly close to the red sequence and were characterized by Bell et al. (2003) to have red colors. The overall spread in colors of field galaxies is much larger (1.5 mag) compared to the spread found here (0.3 mag).

5. DISCUSSION

On the basis of our high-S/N spectra we have found a rather wide range in *M/L* for early-type galaxies at $z = 1$, indicating a range in star formation histories. The *M/L* and colors are well correlated, as expected from stellar population models. Hence, the scatter in *M/L* is real.

The results agree surprisingly well with earlier results based on lensing galaxies. Rusin et al. (2003) and van de Ven et al. (2003) found a range in *M/L*, and van de Ven et al. (2003) found a similar correlation between rest-frame colors and *M/L*. Other authors found either low *M/L* (e.g., Treu et al. 2002; Gebhardt et al. 2003) or high *M/L* (e.g., van Dokkum & Ellis 2003), and this is most likely due to (still unexplained) sample selection effects. The last authors found that galaxies with residuals from the $r^{1/4}$ profile had young ages. However, we find no such relation in our sample.

Stellar population models indicate that the low *M/L* of the blue $z \approx 1$ galaxies may be due to an age difference of a factor of 3. Alternatively, bursts involving 20%–30% of the mass can produce similar offsets. The current sample is too small to determine the fraction of young early-type galaxies at $z \approx 1$ reliably. Large, mass-selected samples are needed for this, as current samples are generally optically selected and therefore biased toward galaxies with lower *M/L*.

It is striking that the most massive galaxies have modest evolution in *M/L*, similar to what van Dokkum & Stanford (2003) found for massive cluster galaxies. The evolution of the galaxies with $M = 6.07 r_e \sigma^2 \geq 3 \times 10^{11}\ M_\odot$ (Jørgensen et al. 1996) in our sample is $\Delta \ln (M/L_B) = (-1.17 \pm 0.14)z$. The implied formation redshift is above 2, ignoring the effects of progenitor bias (van Dokkum & Franx 2001). The mass limit is comparable to the M_* mass of an early-type galaxy: if we take the σ_* of early-type galaxies derived by Kochanek (1994) of 225 km s^{-2}, we derive a typical mass of $M_* = 3.1 \times 10^{11}\ M_\odot$, based on the sample measured by Faber et al. 1989. The sample as a whole evolves as $\Delta \ln (M/L_B) = (-1.64 \pm 0.45)z$, whereas the sample with masses smaller than $3 \times 10^{11}\ M_\odot$ evolves as $\Delta \ln (M/L_B) = (-1.95 \pm 0.29)z$.

The results are therefore consistent with little or no (recent) star formation in massive early-type galaxies out to $z = 1$, and younger populations in less massive galaxies, possibly caused by bursts involving up to 30% of the stellar mass. Since these less massive galaxies have much more regular stellar populations at $z < 0.5$ without signs of recent star formation, these results are consistent with the downsizing seen in the field population (Cowie et al. 1996): at progressively higher redshifts, more and more massive galaxies are undergoing strong star formation.

It remains to be seen how this trend continues out to even higher redshifts. The biases inherent in studies of galaxies at $z = 2$ and higher make it very hard to perform similar studies: the optical light has shifted to the near-IR, and spectroscopy is extremely hard at those wavelengths.

More studies at redshift $z \approx 1$ are needed to determine the distribution of colors and *M/L* of the progenitors of field early-types. Such a determination should be based on mass-selected samples. Further studies of spectral energy distributions extending to the rest-frame infrared will be very useful to better constrain the star formation histories of the bluer galaxies.

We thank the ESO staff for their support during the observations. We thank C. Wolf for making available the COMBO-17 catalog.

REFERENCES

Bell, E. F., et al. 2003, ApJ, submitted (astro-ph/0303394)
Bruzual A., G., Charlot, S. 2003, MNRAS, 344, 1000
Coleman, G. D., Wu, C.-C., Weedman, D. W. 1980, ApJS, 43, 393
Cowie, L. L., Songaila, A., Hu, E. M., & Cohen, J. G. 1996, AJ, 112, 839
Diaferio, A., Kauffmann, G., Balogh, M. L., White, S. D. M., Schade, D., & Ellingson, E. 2001, MNRAS, 323, 999
Faber, S. M., Wegner, G., Burstein, D., Davies, R. L., Dressler, A., Lynden-Bell, D., & Terlevich, R. L. 1989, ApJS, 69, 763
Fisher, D., Fabricant, D., Franx, M., & van Dokkum, P. 1998, ApJ, 498, 195
Franx, M. 1993, PASP, 105, 1058
Gebhardt, K., et al. 2003, ApJ, 597, 239
Jørgensen, I., Franx, M., & Kjærgaard, P. 1995a, MNRAS, 273, 1079
———. 1995b, MNRAS, 276, 1341
———. 1996, MNRAS, 280, 167
Kochanek, C. S. 1994, ApJ, 436, 56
Kochanek, C. S., et al. 2000, ApJ, 543, 131
Rusin, D., et al. 2003, ApJ, 587, 143
Salpeter, E. E. 1955, ApJ, 121, 161
Schlegel, D. J., Finkbeiner, D. P., & Davis, M. 1998, ApJ, 500, 525
Treu, T., Stiavelli, M., Bertin, G., Casertano, S., & Møller, P. 2001, MNRAS, 326, 237
Treu, T., Stiavelli, M., Casertano, S., Møller, P., & Bertin, G. 2002, ApJ, 564, L13
van de Ven, P. M., van Dokkum, P. G., & Franx, M. 2003, MNRAS, 344, 924
van Dokkum, P. G., & Ellis, R. S. 2003, ApJ, 592, L53
van Dokkum, P. G., & Franx, M. 1996, MNRAS, 281, 985
———. 2001, ApJ, 553, 90
van Dokkum, P. G., Franx, M., Kelson, D. D., & Illingworth, G. D. 1998, ApJ, 504, L17
———. 2001, ApJ, 553, L39
van Dokkum, P. G., & Stanford, S. A. 2003, ApJ, 585, 78
Wolf, C., Meisenheimer, K., Rix, H.-W., Borch, A., Dye, S., & Kleinheinrich, M. 2003 A&A, 401, 73